ICAS 2021 SHANG HAI
International Council of the Aeronautical Sciences
32nd Congress of the International Council of the Aeronautical Sciences
September 6-10, 2021
Pudong Shangri-La, Shanghai, China

Multi-objective aerodynamic optimization of a civil aircraft winglet

M. Heidari Soreshjani[1], A. Jahangirian[2, a]

[1]Aerospace Engineering Department, Amirkabir University of Technology, 424 Hafez Avenue, Tehran, Iran.
[a]ajahan@aut.ac.ir

Abstract

A multi-objective aerodynamic optimization of a blended winglet is presented. The objective functions are drag coefficient and wing root bending moment coefficient that are going to be minimized. Furthermore, there is a strict constraint on the Cl value at 0.68 to get the required lift of the aircraft at cruise conditions. The flow is simulated using the Reynolds Averaged Navier–Stokes equations coupled with the k–ω SST turbulence model to study the three-dimensional flow and vortex structure about the winglet. A Multi-Objective Genetic Algorithm optimizer was coupled with the flow solver for calculating the global optima. Finally, two optimum candidates are represented based on the stated objectives. Both candidate points have satisfied the lift coefficient constraint. Comparing the first candidate point to the initial wing shows that we had a drop of 15.1% in drag coefficient, resulting in about a 15.5% increase in aerodynamic efficiency (Cl/Cd). It is noteworthy that this increase in aerodynamic efficiency has been obtained simultaneously with about 11% increase in wing root bending moment while the initial winglet had a drop of about 6.5% in drag and simultaneously about 19.8% increase in bending moments as compared to the initial wing. Results also show that the best candidate point had a drop of 9.7% in the drag coefficient compared to the initial winglet. The Cl/Cd of this candidate is about 2.1% higher than the initial winglet, with about 8.8% lower bending moments.

Keywords: Multi-objective optimization, aerodynamic, winglet parameterization, CFD

1. Introduction

Wing-tip vortices have a significant effect on the aerodynamic efficiency of civil aircraft. These vortices induce downwash on the wing and consequently reduce the angle of attack. This angle of attack reduction inclines the lift vector backward and causes induced drag. Such a phenomenon can create significant efficiency issues for the entire aircraft. Aircraft designers use winglets to fix this problem. These devices reduce an aircraft's drag by partial recovery of the tip vortex energy and decrease the lift-induced drag caused by wing-tip vortices. Winglets also increase the lift generated at the wing-tip without significantly increasing the wingspan. Therefore, the use of winglets can lead to a dramatic increase in wing aerodynamic efficiency.

Over the last decades, especially after the cost of jet fuel skyrocketed in the 1973 oil crisis, engineers have dealt with the problem of induced drag reduction by designing various types of wing-tip extensions. First, some attempts were made by adding vertical flat plates at the wing-tip to prevent the tip vortices formation. However, in the early years, any induced drag reduction never showed its effectiveness in practice. Because the increase in drag due to skin friction and flow separation outweighed any lift-induced drag benefit [1].

In July 1976, Dr. Whitcomb researched NASA Langley's research center and developed the concept of winglet technology [1]. Whitcomb's analysis of flow phenomena at the tip showed that the airflow about the wing-tip of the typical aircraft in flight is characterized by a flow that is directed inward above the wing-tip and a flow that is directed outward below the wing-tip. His analysis led him to hypothesize that a near-vertical, wing-like surface at the wing-tip could indeed reduce the strength of trailing vortices if properly designed. He envisioned that they would extend above and, in some instances, below each wing-tip. A proper design would require a balance between cant, the winglet's angle off vertical, and twist, the angle the winglet deviates from airflow [2]. Whitcomb designed a winglet using an advanced airfoil integrated into a swept, tapered planform that would interact with the wing-tip

airflow to reduce drag. In Whitcomb's report, published in 1976, he found that previous experimenters had primarily observed the fact that winglets would create more significant moments on the wings, requiring heavier wing-support structures to accommodate. One must be careful that flow separation did not occur at any critical speeds, either on the winglet surface or at the winglet-wing junction [3].

In 1994 Aviation Partners Inc. developed an advanced design of winglets called blended winglet. Louis B. Gratzer [4] has the patent for blended winglet. Blended winglets are merely designed to arise (or blend) naturally out of the wing in a smooth fashion to reduce interference drag at the wing-winglet junction, as seen in Whitcomb's winglet. Aviation Partners Inc. and Boeing Company made a collaboration in 1999 for the design of advanced blended winglets. The developed winglets were retrofitted in B737.

Many parameters influence the design of the blended winglets. Length and cant angle are two of the most significant parameters impacting the winglet performance [5]. As a general rule, the larger the length of the added device, the more significant the reduction in induced drag, but that improvement is partially limited by the increase in other drag components such as viscous or wave drag. Moreover, adding a wing-tip device increases the structural loads, particularly the bending moments, resulting in added weight due to the necessary wing reinforcement and the winglet weight itself. As Takenaka et al. [5] showed, high cant angles lead to increased interference and increased wave drag, even when blending is present but reduces the wing bending moments, hence the weight. On the other hand, low cant angle winglets add to the total lift and allow the aircraft to fly at a lower angle of attack, thereby reducing its induced drag but at the cost of higher bending moments. The choice of these two parameters results from a trade-off between different drag components and structural weight.

The twist angle controls overall loading on the winglet and affects the load distribution on the main wing. Because of the inflow angle at the upper wing-tip, the winglet must be twisted out to reduce its effective angle of attack. It also leads to that the winglet starts to stall after the wing stalls. The optimal twist-out angle depends on the inflow angle at the tip and the required winglet angle of attack for optimal span-wise lift distribution, corresponding to the minimum induced drag. The Boeing 737NG winglets were first designed without a twist-out angle, which resulted in high induced drag reductions but high bending loads. The winglet was later twisted out 2 degrees to reduce the loads; this increased the induced drag but decreased other drag components such as wave and profile drag, compensating the induced drag benefit loss [6]. Additional twist can be added to the winglet to achieve the desired lift distribution but is not generally required [1].

For aerodynamic efficiency, the winglet must be tapered in the same way a wing would be [1]. Also, the winglet sweep has effects on tailoring the load distribution. It can be similar to that of the original wing not to alter its effectiveness in its flight condition.

In the blended winglets, the junction between the wing and winglet is significantly rounded ("blended"). There is no discontinuous change in chord within the blending region, and the chord decreases smoothly. The use of a large smooth fillet between the wing-tip and winglet root reduces the induced drag benefit compared to a sharp canted winglet [7], but the benefits in terms of viscous drag and reduced interference [7, 8].

Finally, it should be mentioned that all these critical parameters affect winglet aerodynamic performance, and it is so complicated to take into account their effects simultaneously in winglet design. That is where CFD could help by enabling fast parametric configuration studies, and these CFD computations should be coupled with an optimization method to achieve optimum design parameters. In this work, the use of a blended type winglet appeared as a good choice for retrofitting a regional jet due to its simplicity and to the fact that this concept has been successfully used for many aircraft, especially in similar aircraft classes.

2. Winglet shape modeling and parameterization

Modeling and parameterization are the first steps in engineering optimization. It is essential for modeling to have the ability to reproduce new geometries quickly, in an automated way, without failure, and to be flexible enough to generate diverse geometries. To get these features, we use ANSYS Design Modeler, which is a parametric feature-based solid modeler.

As shown in figure 1, the blended winglet is modeled in four segments in which all segment joints are in a unified direction:

1- Wing extension
2- Transition segment
3- Winglet
4- Winglet cap

The wing extension keeps the same wing taper ratio. The transition segment connects the wing extension smoothly to the main body of the winglet. In this segment, wing-tip airfoil also changes to a symmetric airfoil. At the end of the transition segment, the body of the winglet extends with specific features. Finally, a cap inspired by the conventional blended winglets fills the end of the winglet segment.

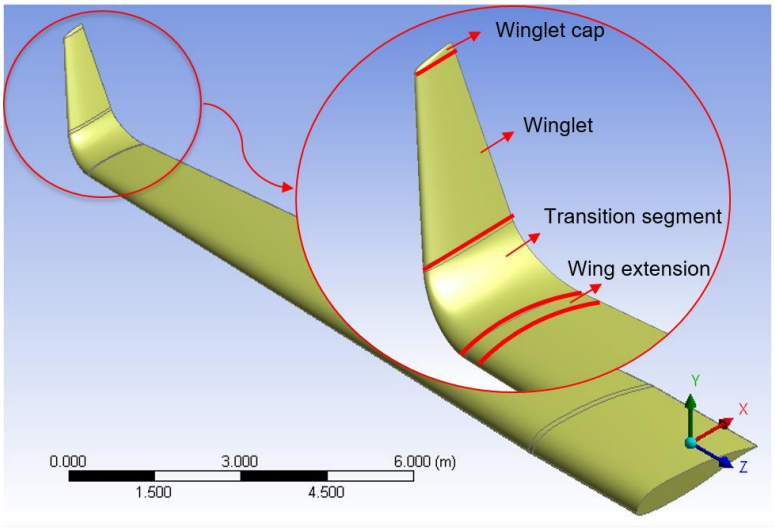

Figure 1 - Wing and initial winglet configuration.

Parameterization helps to execute a set of operations repeatedly with a different set of values. Important features, such as lengths, angles, and diameter of the fairing, can be made parametric. The parameters can be linked with design exploration to perform a direct optimization.

In this modeling, the blended winglet geometry is parameterized with six parameters (Figure 2):

1- Winglet length
2- Sweep back
3- Cant angle
4- Taper ratio
5- Twist angle
6- Radius of transition

To maintain the lift distribution unchanged, it may be necessary to adjust parameters such as the angle of attack. So, in this optimization, the angle of attack is selected as the 7th parameter. **Error! Reference source not found.** indicates the lower and upper bound for each input parameter. A wide range is defined for every parameter in this optimization to ensure no intervals have been lost.

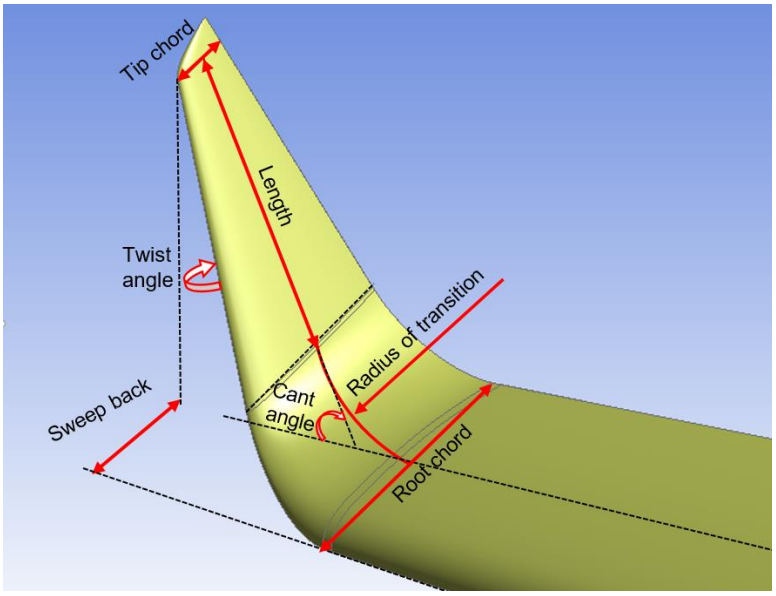

Figure 2 - Geometric parameters of the blended winglet.

Table 1 - PARSEC parameters and their boundaries.

Name	Lower Bound	Upper Bound
Sweep Back (m)	0.7	2
Cant Angle (degree)	45	80
Length (m)	0.5	2
Transition Radius (m)	0.8	1.4
Taper Ratio	0.15	0.4
Twist Angle (degree)	-10	0
Angle of Attack (degree)	1	2

3. Mesh Generation

The grid significantly impacts solution accuracy, the CPU time required, and convergence rate (or lack of convergence). In this project, we construct a hemisphere at a radius of 100 meters for the fluid domain. A high-quality hybrid mesh is generated to capture the flow details, especially in critical regions around the winglet. Figure 3 indicates the generated mesh for the fluid domain, which is achieved by applying boundary layer inflation mesh near solid walls, and tetrahedral mesh to fill the rest of the domain. The generated mesh has 1718577 nodes and 5704685 elements with a maximum skewness of 0.94. This mesh can be generated quickly and automatically for new geometries generated during the optimization process.

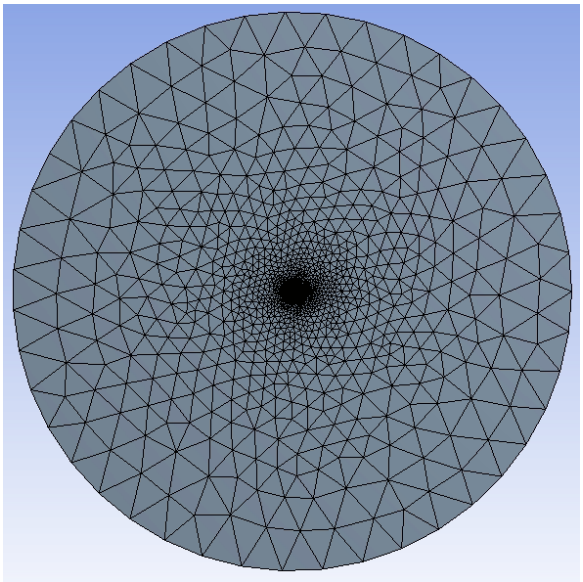

a. Overview

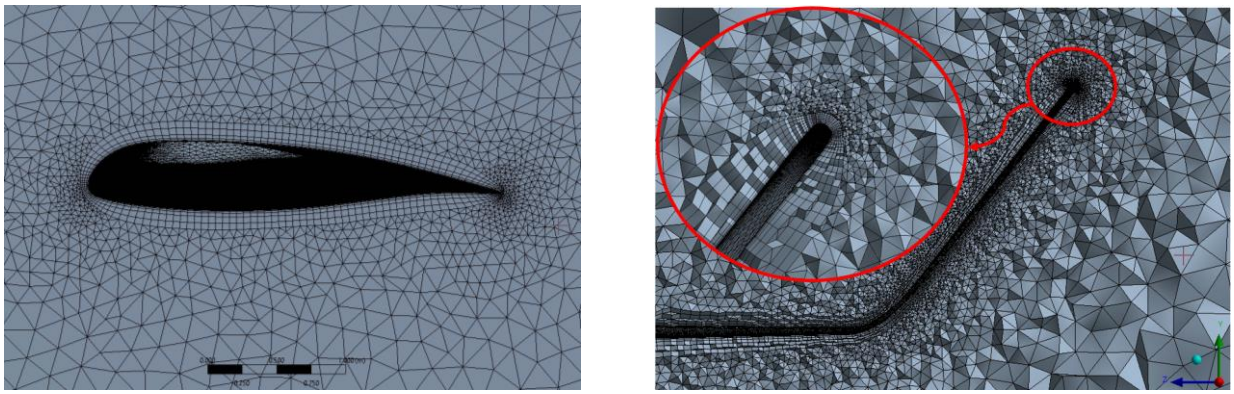

b. Close up c. Cross-section

Figure 3 - The generated mesh for the fluid domain.

4. Objective Function Evaluation by CFD

Computational Fluid Dynamics (CFD) is a computer-based tool for simulating the behavior of fluid flow. It works by solving the equations of fluid flow (in a particular form) over a region of interest, with specified boundary conditions. The equations describing momentum, heat, and mass transfer are known as the Navier-Stokes equations. ANSYS CFX solves these unsteady equations in their conservation form. k-omega SST is used as a turbulence model in this project to accurately predict the onset and the amount of flow separation under adverse pressure gradients. The equations relating to fluid flow are closed numerically by the specification of conditions on a domain's external boundaries. It is essential to set boundary conditions that accurately reflect the actual situation to obtain accurate results. For this purpose, we define four boundary conditions as follows:

1- Inlet: Fluid just can flow into the domain.
2- Opening: Fluid can flow both in and out of the domain.
3- Symmetry Plane: A plane of both geometric and flow symmetry.
4- Wall: Impenetrable boundary to fluid flow.

Figure 4 indicates how these boundary conditions applied to external boundaries of the domain.

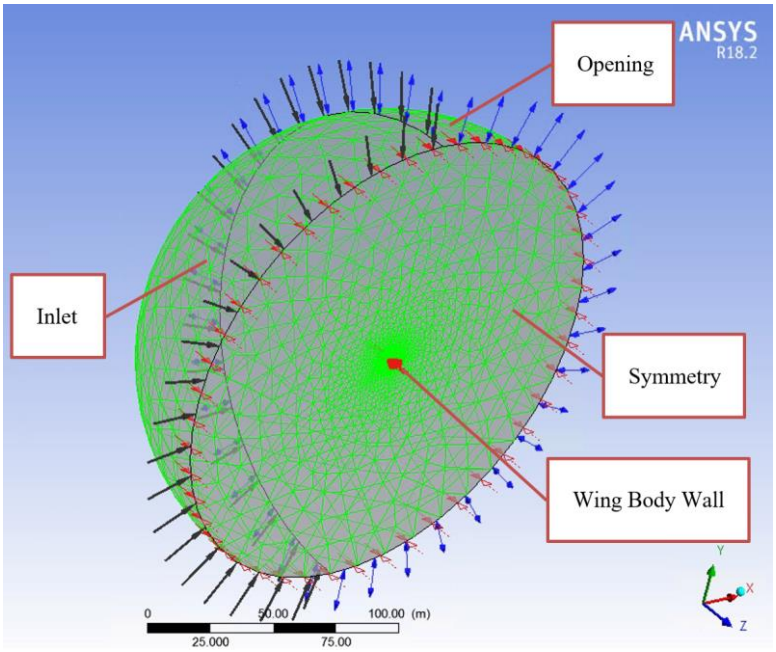

Figure 4 - Boundary conditions.

5. Optimization

5.1. objectives and Constraints

In this work, two objective functions are considered for aerodynamic optimization of a regional jet winglet:

1- Minimize Cd
2- Minimize Cm

Minimizing Cd is the main objective and has higher importance and minimize Cm is a secondary objective with lower importance that will be imposed to minimize structural costs. Furthermore, there is a strict constraint on Cl value, and it should be greater than or equals to 0.68, as requested by the employer.

5.2. Optimization Method

Multi-objective optimization techniques find the "best" possible designs are obtained from a sample set given the objectives. A good design point is often the result of a trade-off between various objectives; hence, exploring a given design cannot be performed using optimization algorithms that lead to a single design point. In this case, the objective functions are conflicting, and there exists a number of Pareto optimal solutions.

Multi-Objective Genetic Algorithm (MOGA) is the most famous multi-objective optimization method for engineering applications, and we use it as the optimization method in this project. The MOGA is a variant of the popular NSGA-II first developed by Kalyanmoy Deb [9]. It supports multiple objectives and constraints and aims at finding the global optimum.

There are different settings in this project to define the optimization problem. In this optimization, the number of initial samples and number of samples per iteration will be 100 and 50, respectively. The fewer number in each case can lead to local optimum. Furthermore, default settings for maximum allowable Pareto percentage and convergence stability percentage will be preserved as convergence criteria. Also, we set the maximum number of iterations 20 as stopping criteria. Table shows the summary of optimization settings.

Table 2 - Optimization settings.

Method Name	MOGA
Number of Initial Samples	100
Number of Samples Per Iteration	50
Maximum Allowable Pareto Percentage	70
Convergence Stability Percentage	2
Maximum Number of Iterations	20
Maximum Number of Candidates	6

5.3. Optimization Results

The optimization process converged after seven iterations due to convergence stability percentage criteria. MOGA generated 393 CFD evaluations in these iterations and represented two optimum candidates. The best candidates are obtained from ranking the solution by an aggregated weighted method. Table 3 indicates these candidate points compared to the initial wing and initial winglet at an angle of attack of 2 degrees. As can be seen, the initial wing has a Cd of 0.0291, while this value decreases by 6.53 percent to 0.0272 for the initial winglet. The initial wing Cl and Cm are 0.6972, and 0.2734 and these values increase by 13.43 and 19.82 percent for the initial winglet. However, all candidate points have satisfied the lift coefficient constraint, and they have near 0.68 lift coefficient. This constraint means that they have been allowed to reduce the lift coefficient by about 8 percent in exchange for a significant drop in the drag coefficient. So candidate points 1 and 2 had a significant drop of 15.12 and 14.43 percent in drag coefficient, respectively. This means that they have about 8-9 percent lower drag coefficient compared to the initial winglet. In addition, these candidate points' aerodynamic efficiency (Cl/Cd) has increased by 15.48 and 14.15 percent compared to the initial wing. It should be noted that this increase in aerodynamic efficiency has been obtained simultaneously with

an increase in bending moments of 11.04 and 8.96 percent, which is much less than the increase in the initial winglet bending moment.

A noteworthy point in comparing the two candidates is that despite the superior aerodynamic performance of the first candidate, the second candidate has a structural advantage and imposes approximately 2% less bending moment on the wing. This feature is mainly obtained due to the lower length, cant, twist, and angle of attack of the second candidate compared to the first candidate. Figure 5 indicates initial wing and winglet geometries compared to the two candidate points and their surface total pressure contour. As can be seen, the pressure contours are different as their geometries are entirely different.

Table 3 - Comparison of the parameters and results for the initial wing and the best candidate points.

	Initial Wing	Initial Winglet	Candidate Point 1	Candidate Point 2
Sweep Back (m)	-	1.4	1.43	1.94
Cant Angle (degree)	-	62	56.66	52.83
Length (m)	-	1.55	0.91	0.88
Transition Radius (m)	-	0.5	1.12	1.01
Taper Ratio	-	0.33	0.18	0.17
Twist Angle (degree)	-	0	-1.29	-4.02
Angle of Attack (degree)	2	2	1.25	1.17
Cd	0.0291	0.0272	0.0247	0.0249
Cd decrease	-	6.53 %	15.12 %	14.43 %
Cl	0.6972	0.7380	0.6836	0.6809
Cl/Cd	23.96	27.18	27.68	27.35
Cl/Cd Increase	-	13.43 %	15.48 %	14.15 %
Cm_x	0.2734	0.3276	0.3036	0.2979
Cm_x Increase	-	19.82 %	11.04 %	8.96 %

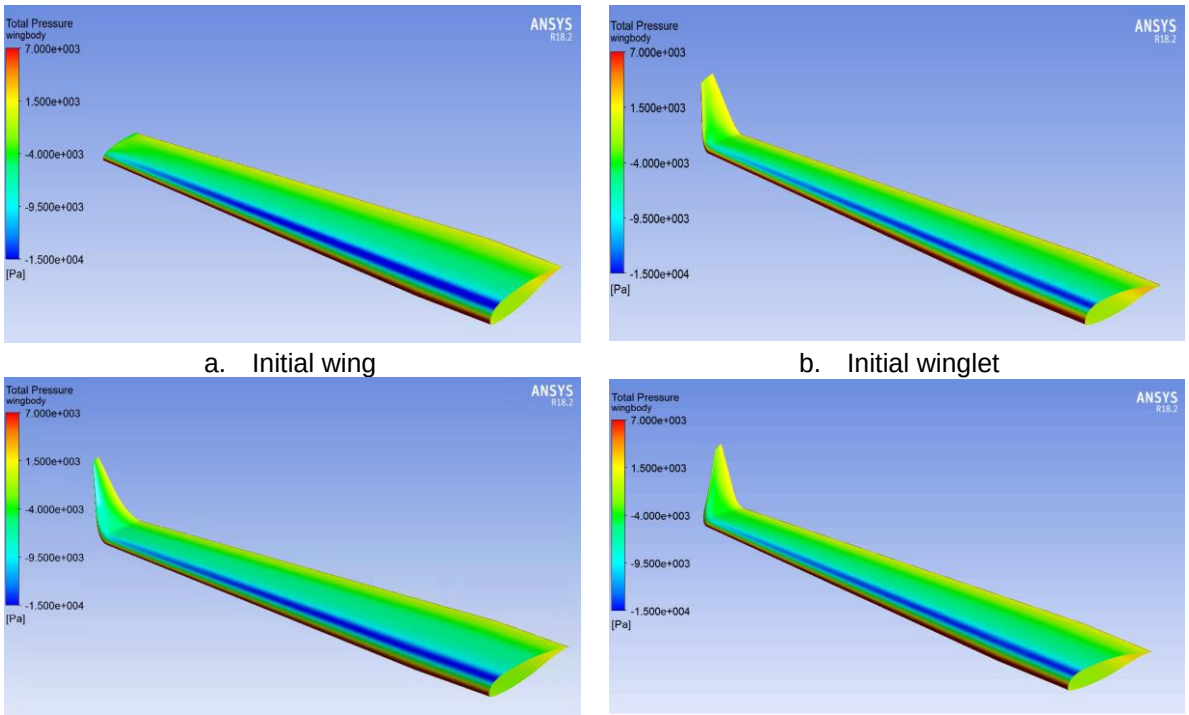

a. Initial wing b. Initial winglet

c. First candidate point d. Second candidate point

Figure 5 - Total pressure contour of different configurations.

Turbulent vertical structures of the flow field are visualized in Figure 6. This figure shows the iso-surface with an actual vorticity value of 50 [s^-1] that is colored with velocity in the flow field at the rear of the wing and under the cruise condition. The wake vorticity produced by the wing-tip of the initial wing is quite large and constitutes an additional drag (induced drag) that does not quickly dissipate. Both the

wing with an initial winglet and two candidate points reduce the wake vorticity and effectively diffuse the vortex core, which helps to reduce the vortex wake of an airplane. The first candidate point configuration primarily distributes its vorticity more evenly than the initial winglet configuration and has better aerodynamic efficiency.

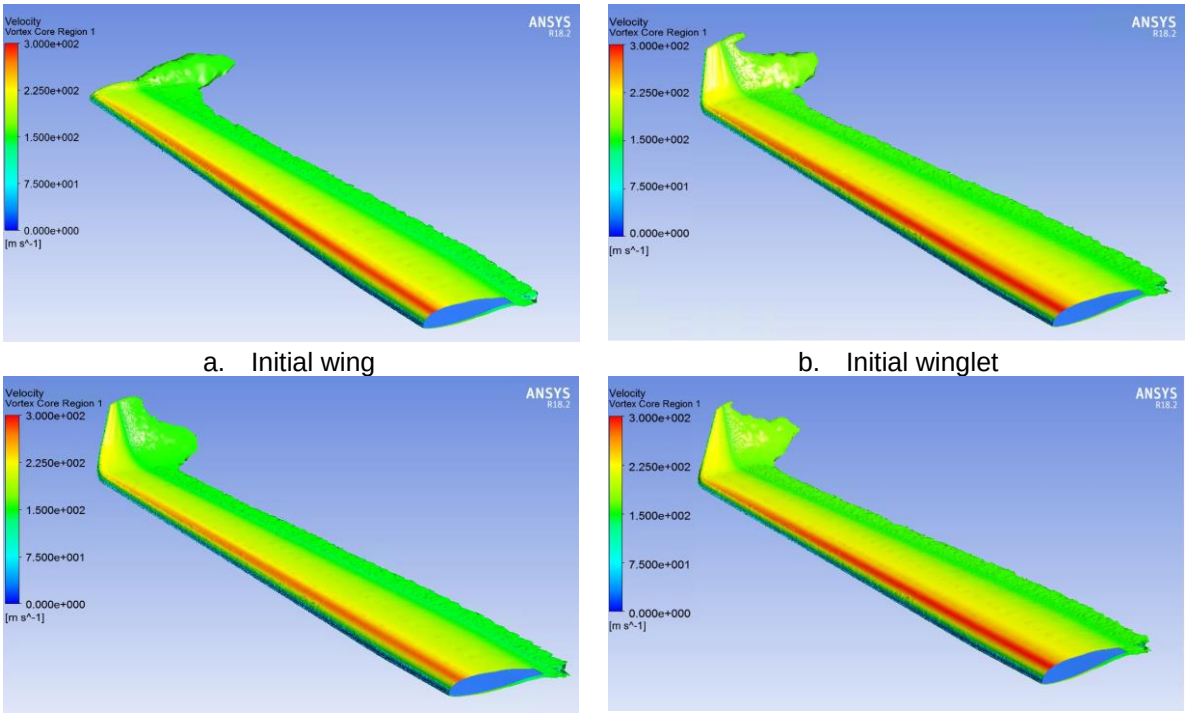

a. Initial wing b. Initial winglet

c. First candidate point d. Second candidate point

Figure 6 - Vortex core region of different configurations.

Figure 7 shows the trade-off study of Cd against Cm performed on the MOGA sample set. In this chart, the samples are ranked by non-dominated Pareto fronts. The first Pareto front (non-dominated solutions) is shown as blue points on the output-axis plot. Also, Pareto front 2, 3, and 4 are shown with green, yellow, and pink points. This shows which goals can be achieved and whether this entails sacrificing the goal attainment of other outputs.

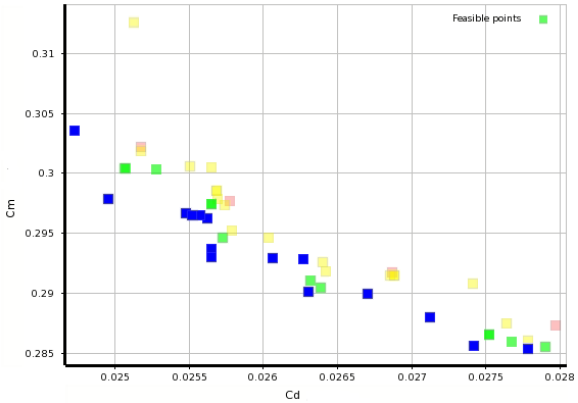

Figure 7 - Trade-off chart Cd vs. Cm.

6. Conclusions

In winglet optimization, the objective functions are conflicting, and the optimum design results from a trade-off between various objectives. Therefore, in this project, optimization was done with the help of MOGA. The results showed that the initial wing forms a strong vortex, somewhat weakened by the initial winglet. However, the aerodynamic performance of the top candidates was significantly improved compared to the initial winglet. Equipping the wing to the best candidate point drops 8.6% of the drag coefficient compared to the initial winglet. Cl/Cd of this candidate is about 2.1% higher than the initial winglet, with about 8.8% lower bending moments. In addition, the second candidate of multi-objective

optimization has an aerodynamic performance close to the first candidate and at the same time has about 2% less bending moment coefficient.

Copyright Statement

References

[1] Whitcomb R.T. A design approach and selected wind tunnel results at high subsonic speeds for wing-tip mounted winglets. Washington, DC: NASA TN D-8260, 1976.

[2] Hallion R. NASA's Contributions to Aeronautics. National Aeronautics and Space Administration, 2010.

[3] Chambers J.R. Concept to reality: contributions of the Langley Research Center to US Civil Aircraft of the 1990s, 2003.

[4] Gratzer LB. Blended Winglet, United States Patent Document, Patent No. US5348253 A, 1993.

[5] Takenaka K, Hatanaka K, Yamazaki W and Nakahashi K. Multidisciplinary design exploration for a winglet. Journal of Aircraft, Vol. 45, No. 5, 2008.

[6] Faye R, Laprete R, and Winter M. Blended winglets for improved aircraft performance. In Aero magazine (p. 16-31). Boeing, 2002.

[7] McLean D. Wing-tip devices: What they do and how they do it. Performance and Flight Operations Engineering Conference, 2005.

[8] Thomas A.S. Aircraft drag reduction technology - a summary [AGARD Report No.723]. In Aircraft drag prediction and reduction, 1985.

[9] Deb K, Pratap A, Agarwal S and Meyarivan T. A fast and elitist multi-objective genetic algorithm: NSGA-II, IEEE Transactions on Evolutionary Computation, Vol. 6, No. 2, 2002.